

1

2 **Direct Evidence of a Changing Fall-rate Bias in XBTs**  
3 **Manufactured During 1986-2008**

4

5 Pedro N. DiNezio<sup>1,2 \*</sup>

6 Gustavo J. Goni<sup>2</sup>

7

8 <sup>1</sup>Cooperative Institute for Marine and Atmospheric Studies, University of Miami, Miami,  
9 Florida

10 <sup>2</sup>NOAA/Atlantic Oceanographic and Meteorological Laboratory, Miami, Florida

11

12 *Submitted to Journal of Atmospheric and Oceanic Technology*

13 1/31/2011

14

15 \* Pedro N. DiNezio, Cooperative Institute for Marine and Atmospheric Studies, Rosenstiel School of  
16 Marine and Atmospheric Science, University of Miami, 4600 Rickenbacker Causeway, Miami, FL 33149.

17 E-mail: [pedro.dinezio@noaa.gov](mailto:pedro.dinezio@noaa.gov)

18

19

## Abstract

Results from an experiment performed in order to determine whether there is a year-dependent fall-rate bias in eXpendable BathyThermographs (XBTs) are presented. A total of 52 temperature profiles collected with same recording system and under the same ocean conditions, but with XBTs manufactured during years 1986, 1990, 1991, 1995, and 2008 are analyzed. These profiles are compared with co-located profiles obtained from Conductivity Temperature Depth (CTD) casts using a methodology that unambiguously separates depth errors from temperature errors. We find systematic depth errors linearly increasing with depth consistent with a fall-rate bias. According to the manufacture date of the probes, this fall-rate has changed from  $(-3.77 \pm 0.57)$  % of depth in 1986 to  $(-1.05 \pm 1.34)$  % of depth in 2008. The year dependence of the fall-rate bias can be identified with statistical significance ( $1\sigma$ ) below 500 m, where the effect of the fall-rate bias is larger. This result is the first direct evidence of changes in the XBT fall-rate characteristics. Therefore, for the 1986-2008 period, the hypothesis that the XBT errors are due to a time-varying fall-rate bias, as hypothesized by Wijfels et al. (2008), cannot be rejected. Additional implications for current efforts to correct the historical temperature profile database are discussed.

## 37 Introduction

38 EXpendable BathyThermographs (XBTs) are widely used to observe the upper  
39 ocean from ships of opportunity due to their low cost and ease of use. Until the  
40 completion of the Argo array in 2005, more than 50% of all temperature profile  
41 observations were collected using XBTs. These profiles are a fundamental source of  
42 information about ocean changes during much of the observational record. Unlike more  
43 costly instruments equipped with pressure sensors, such as Conductivity Temperature  
44 Depth (CTD) casts or profiling floats, XBTs determine the depth of the temperature  
45 observations indirectly using a fall-rate equation (FRE).

46 Systematic errors in the computed XBT depths have been identified since the mid  
47 1970s (e.g. Seaver and Kuleshov 1982; Roemmich and Cornuelle 1987), but their impact  
48 on climate applications was recognized only in the 1990s, after a comprehensive analysis  
49 of research-quality CTD and XBT data from several regions of the world ocean (Hanawa  
50 et al. 1995, hereinafter H95). H95 study showed that the coefficients in the FRE used at  
51 that time resulted in isotherm depths that were too shallow, producing a ‘cold’  
52 temperature bias in most of the water column.

53 This issue has regained importance after Gouretski and Koltermann (2007) found  
54 a year-dependent “warm” temperature bias by globally comparing climatologies derived  
55 from XBT and CTD/bottle observations. This result was later confirmed and attributed to  
56 changes in fall-rate characteristics of the XBT probe due to minor manufacturing changes  
57 over time (Wijffels et al. 2008). Removing this year-dependent bias has improved the  
58 detection of decadal variability and long-term trends in ocean heat storage (e.g. Wijffels

et al. 2008; Levitus et al. 2009; Ishii and Kimoto 2009) and sea level (Domingues et al. 2008).

However, the origin of the XBT errors is still unclear because there is an alternative explanation for the year-dependence of the warm biases. A more recent study comparing the same XBT and CTD climatologies shows that the year-dependent XBT “warm” bias might be explained as a superposition of a constant fall-rate bias plus a year-dependent ‘pure’ thermal bias (Gouretski and Reseghetti 2010). This is an important issue not only because past XBT data need to be adequately corrected, but also because the origin of the errors needs to be identified prior to any attempt to improve the XBT technology.

These studies have examined the year-dependence and origin of XBT biases comparing XBT and CTD climatologies. However, because the ocean is thermally stratified, depth errors and pure thermal errors can be confounded. For this reason a definitive answer on this issue will remain elusive if this methodology is used. In contrast, comparing co-located XBT/CTD profiles is the most reliable way to isolate depth errors in XBTs. The vertical temperature gradient of the co-located profiles, which are free from ‘pure’ temperature errors, can be compared to directly estimate depth errors.

In this study we apply this methodology to co-located profiles collected using XBTs manufactured in years 1986, 1990, 1991, 1995, and 2008, but from the same ocean conditions. Using XBTs with different manufacture dates allows us to evaluate whether the XBT fall-rate bias has changed because of manufacture changes during the last 25 years. The profiles were collected in the tropical North Atlantic, a region where layers of

homogeneous temperature with a “stair-case” structure facilitate the detection of vertical temperature gradients and hence depth errors. Our results are the first direct evidence of changes in the XBT fall-rate bias during 1986-2008 supporting previous results obtained by comparing climatologies (Wijffels et al. 2008; DiNezio and Goni 2010).

## 1. Data and Methods

### *a) Data*

A total of 52 high quality co-located XBT and CTD temperature profiles used in this study were collected in the tropical North Atlantic (Figure 1) from 11 July – 11 August 2009 during the PIRATA Northeast Extension 2009 (PNE09) cruise. All the XBTs used in this experiment were manufactured by Lockheed Martin Sippican (hereinafter Sippican), and obtained using the same data acquisition system consisting of a Sippican handlauncher model LM-3A, a Mk12 recorder, and a computer. The XBTs were dropped from about 2.5 m, the launching height specified by Sippican to minimize the effect of hydrodynamical transients when the probe enters the ocean. Good weather conditions and a very calm sea state prevailed throughout the duration of these co-located casts, contributing to minimizing surface transients.

The major difference among the XBT profiles obtained in this experiment is the manufacture date of the probes. Another possible difference could result from the fact that we used different XBT models. XBTs manufactured between 1986 and 1995 are model T7 and the XBTs manufactured in 2008 are model DeepBlue (DB). However, these models use the same FRE because the hydrodynamical properties of the XBT probe, such as drag and weight, are the same. Both T7 and DB reach about 750 m, and

104 constitute more than 50% of the XBT archive during the 1990-2010 period. Out of the 40  
105 T7 XBTs deployed in the experiment, 19 were manufactured on 4/1/1986, with serial  
106 numbers in the ranges 552664-552674 and 552748-552759, 21 were manufactured  
107 between 1990 and 1995 (1 in 8/3/90 with serial number 695092, 8 in 4/23/91 with serial  
108 numbers in the range 727812-727823, and 12 in 7/11/1995 with serial numbers in the  
109 range 897565-897576). The remaining 12 XBTs were DB model manufactured in  
110 11/26/2008, with serial numbers in the range 1085470-1085793.

111 The XBT measures temperature as a function of time elapsed since the XBT hits  
112 the water surface,  $t$ , which is then converted into depth,  $z_{FRE}$  using the FRE:

113 
$$z_{FRE} = At - Bt^2 . \quad (1)$$

114 The  $A$  and  $B$  coefficients in (1) are semi-empirical constants related to the  
115 hydrodynamics of the probe descent. The  $A$  coefficient represents the value of the  
116 terminal velocity of the probe, or fall-rate, and is, to first-order, determined by the drag  
117 coefficient and by the mass of the probe in the water. The deceleration term,  $-Bt^2$ ,  
118 accounts for the reduction of probe mass as the wire pays out and for the increasing drag  
119 with depth (Green 1984). We calculated the XBT depths,  $z_{FRE}$ , using the FRE (1) with the  
120 original Sippican coefficients  $A = 6.472 \text{ ms}^{-1}$  and  $B = 216 \times 10^{-5} \text{ ms}^{-2}$ , i.e. without the  
121 stretching factor applied to the FRE after the study of H95.

122 The XBTs used in this experiment had been stored away from excessive heat,  
123 sunlight, or moisture according to Sippican specifications, along with the XBTs used for  
124 normal operations at NOAA's Atlantic Oceanographic and Atmospheric Laboratory. It is  
125 very likely that the accuracy of the XBT thermistor degraded because the shelf time of 5

years specified by Sippican was exceeded for the XBTs manufactured from 1986 to 1995. This could result in temperature bias. However, the fall-rate characteristics of the probe are not likely to have changed, since they depend on weight, shape, and surface roughness of the probe.

The errors in the XBT profiles are evaluated relative to co-located profiles obtained with a CTD profiler with dual temperature and salinity sensors. The CTD sensors were calibrated 21 May 2009, and the results used to correct the CTD profiles before the comparison with the XBT profiles. A methodology that accounts for the variation of gravity with latitude and depth, and the effect of pressure on density [Saunders, 1981], was used to convert CTD pressure into depth,  $z_{\text{CTD}}$ . This methodology neglects the small influence of salinity and temperature on density with an error less than 0.25 m, which is at least one order of magnitude smaller than the hypothesized biases in XBT depth determined via the FRE equation, which are estimated as about 15 m at 700 m depth.

#### ***b) Method***

Disregarding problems in the recording system, XBT errors originate from: 1) the estimation of depth due to deficiencies of the FRE to capture the true hydrodynamics of the probe, and/or 2) temperature errors due to either the finite time response of the thermistor or inaccuracies in the conversion of resistance to temperature by the recording system. There are two main reasons why the FRE could lead to depth errors: 1) fall-rate errors due to inaccurate  $A$  and  $B$  coefficients resulting from changes in probe weight or drag, and 2) hydrodynamics of the probe descent that depart from the physical model

used to derive the FRE, such as initial transients. Separating depth errors from ‘pure’ temperature errors is not trivial, even when co-located CTD profiles are available.

For instance, one pair of XBT and CTD profiles obtained on the equator at 23°W shows substantial temperature differences (Figure 2a, red and blue lines). Note the large differences at about 250 m, which reach about 1°C, are comparable to, or even larger than, decadal or global warming signals. The true XBT depths could be estimated by comparing the depth of isotherms in the XBT and the CTD profile. This is the method used to estimate depth errors from climatological data (e.g. Wijffels et al. 2008). However, a “pure” temperature bias in the XBTs could introduce a bias in the isotherm depths, even in the absence of depth errors. Differentiating to compute the vertical temperature gradient  $\partial T/\partial z$ , effectively removes ‘pure’ temperature errors that are highly correlated on short vertical lengths. Depth errors can then be estimated by comparing the co-located  $\partial T/\partial z$  profiles. This is the essence of the method implemented by H95 based on previous studies (Hanawa and Yoritaka 1987; Hanawa and Yoshikawa 1991; Hanawa and Yasuda 1992; Rual 1991). Analysis of the vertical temperature gradients  $\partial T/\partial z$ , shows that the  $\partial T/\partial z$  profile obtained from the XBT (Figure 2a, red line) is strikingly similar to that obtained from the CTD (Figure 2a, blue line). Moreover, the XBT signals are clearly shifted upwards at the depths where the temperature differences are largest.

XBT and CTD profiles from the tropical North Atlantic (Figure 2 top), a region where a “stair-case” vertical thermal structure can be found at depths down to about 700 m, is ideally suited to implementing this method because the presence of associated vertical temperature gradients throughout the water column allows the estimation of the true depth of the XBT profiles over the entire depth range. This becomes important to



understanding the FRE bias, because depth errors due to this type of bias are expected to increase with depth.

The procedure to estimate the depth errors in each XBT profile used in this study consists of the following steps:

**a. XBT - CTD pairs.** Each XBT profile is paired with its corresponding CTD profile, collected within 6 hours and 0.1 degrees of distance in longitude or latitude.

**b. Interpolation.** XBT and CTD profiles are linearly interpolated into 1-meter resolution profiles starting at 2 m deep, since some CTD casts do not start collecting data until that depth, down to 800 m, the nominal maximum depth of T7 and DB XBTs.

**c. Filtering.** The interpolated XBT and CTD profiles are smoothed using a second order Butterworth filter with a 5 m low pass cut-off in order to remove small-scale geophysical and instrumental noise (e.g. spikes).

**d. Calculation of temperature gradient.** Profiles of vertical temperature gradient are computed using centered differences at each 1-meter depth from both filtered CTD and XBT data.

**e. Estimation of true XBT depth.** The true depth of the XBT temperature profiles,  $z_{\text{XBT-true}}$ , is obtained by shifting each XBT depth estimated using the FRE,  $z_{\text{FRE}}$ , in order to maximize the correspondence between  $\partial T / \partial z_{\text{XBT}}$  and  $\partial T / \partial z_{\text{CTD}}$ . A 50 m-deep window is centered on each 1-meter depth along the  $\partial T / \partial z_{\text{XBT}}$  profile and then shifted up and down throughout the entire profile until the maximum correlation with the  $\partial T / \partial z_{\text{CTD}}$  profile is found. The entire profile is scanned for correlations because the auto-correlation function of the  $\partial T / \partial z$  profiles decays very rapidly and shows no periodicity (not shown).

The maximum correlations are generally found for shifts no larger than 50 m. The depth at which the shifted  $\partial T/\partial z_{\text{XBT}}$  profile exhibits maximum correlation with the  $\partial T/\partial z_{\text{CTD}}$  profile is the actual depth of the  $\partial T/\partial z_{\text{XBT}}$  profile, and hence of the XBT profile. The value of this maximum correlation is used to evaluate the accuracy of this “true” depth estimation. The CTD depth,  $z_{\text{CTD}}$ , where this correlation is maximum is the actual depth measured by the XBT,  $z_{\text{XBT-true}}$ . We compare this depth with the depth obtained from the FRE,  $z_{\text{FRE}}$ , to study the magnitude and vertical distribution of the XBT depth errors. This procedure adjusts the XBT depths at each 1-m level and within a relatively small window compared with the entire profile depth. Therefore, the XBT depth errors are not forced to fit a given vertical distribution. It is noteworthy, however, that the vertical distribution of the  $z_{\text{XBT-true}}$  minus  $z_{\text{FRE}}$  differences have such evident linear dependence with depth, already anticipating a fall-rate bias (Figure 2d).

The implementation of the methodology to estimate  $z_{\text{XBT-true}}$  from a CTD-XBT pair is illustrated in Figure 2. As discussed above, this pair of XBT and CTD profiles obtained on the equator at 23°W shows substantial temperature differences (Figure 2a, red and blue lines). These differences become more apparent when the vertical gradients are computed (Figure 2b), which show the maxima in  $\partial T/\partial z$  associated with the “stair steps” (see blow-ups of Figure 2a and 1b), generally shifted upwards in the XBT profile (red) compared with the CTD profile (blue). The  $\partial T/\partial z$  profile obtained after adjusting the XBT depths with the CTD data,  $\partial T/\partial z_{\text{XBT-true}}$  (green), shows a surprising correspondence with the  $\partial T/\partial z_{\text{CTD}}$  profile over most of the depth of the XBT profiles. This correspondence is shown by values of the correlation coefficient, after the depth adjustment, exceeding 0.80 down to about 550 m (Figure 2c). As a result of the depth

adjustment, the total correlation between  $\partial T / \partial z_{\text{XBT}}(z)$  and  $\partial T / \partial z_{\text{CTD}}(z)$  from 0.73 to 0.97 for this individual XBT/CTD pair. Note that the correspondence between the CTD and the depth-adjusted XBT profiles is so good that the blue and green lines are indistinguishable (Figure 2a). In general, the adjustment of the XBT depths increases the total correlation between  $\partial T / \partial z_{\text{XBT}}(z)$  and  $\partial T / \partial z_{\text{CTD}}(z)$  in all 52 profiles, with a mean correlation coefficient increasing from  $0.77 \pm 0.13$  to  $0.96 \pm 0.03$  after the depth adjustment (where the uncertainty value is the standard deviation).

For all XBT/CTD pairs, the vertical gradients become increasingly smaller both deeper than 700 m and near the surface, severely limiting the ability of this methodology to estimate the true XBT depths at these depth ranges. In addition, some profiles show low correlation at intermediate depths, such as at 200 m for the 23°W equator profile (Figure 2c). We used the local correlation coefficient of the  $z_{\text{FRE}}$  adjustment to determine the estimates of  $z_{\text{XBT-true}}$  that would be used in the identification and quantification of depth errors presented in the next section. Only true depths estimated from adjusted gradients with a correlation of 0.7 or greater (see step e or Figure 2c) were used to estimate the  $z_{\text{XBT-true}}$ . The conclusions derived from the analysis of the 52 profiles used here do not change when local correlation cut-offs from 0.6 to 0.8 are used. Using  $z_{\text{XBT-true}}$  estimated from highly correlated portions of the XBT and CTD  $\partial T / \partial z$  profiles allows the reduction of the uncertainty in the estimation of the fall-rate bias. Conversely, if a correlation threshold larger than 0.8 is used, the number of  $z_{\text{XBT-true}}$  estimates decreases, resulting in increased uncertainty in the estimation of the fall-rate errors.

**f. Visual QC.** The adjusted vertical gradients (e.g. Figure 2b), the correlation between them, the local correlation between the  $\partial T / \partial z$  profiles (e.g. Figure 2c), and the

depth dependence of the resulting depth differences,  $z_{\text{FRE}}$  minus  $z_{\text{XBT-true}}$ , (e.g. Figure 2d) were visually inspected for all 52 XBT – CTD pairs before proceeding to the analysis of the depth errors as a function of the manufacture date of the XBTs.

**g. Estimation of fall-rate and temperature bias.** Depth and temperature differences for depths ranging from 20 m to 700 m were used to estimate the magnitude of the fall-rate and temperature biases. The methodology used here is unable to detect gradients at depths above and below these limits. The linear depth bias, or ‘fall-rate’ bias, is computed for each individual profile as the least-squares slope of a best-fit straight line adjusting the profile of  $z_{\text{FRE}}$  minus  $z_{\text{XBT-true}}$  differences. The slope is computed assuming that the differences are zero at the surface ( $z = 0$ ). The fall-rate bias is a percentage of depth, because it is the slope between two depth estimates. The ‘pure’ temperature bias is the depth-averaged value of the temperature differences between the depth-adjusted XBT profile ( $T_{\text{XBT}}, z_{\text{XBT-true}}$ ) minus the CTD profile ( $T_{\text{CTD}}, z_{\text{CTD}}$ ) in units of °C.

**h. Systematic errors as a function of manufacture date.** We analyze the temperature profiles (Figure 3, left), the associated depth errors (Figure 3, center), and pure temperature errors (Figure 3, right) for each three groups of XBTs, separated according to their manufacture year: 1986, 1990-1995, and 2008. We also estimate the uncertainty of the fall rate and temperature biases for each of the manufacture years, using the median as the expected value and the range given by the standard deviation among the individual estimates (Table 1, Columns 5, 7, and 8). The median errors avoids the influence of outliers in small sample sizes like these.

## 2. Results

### a) Depth errors

All profiles show depth errors, increasing with depth that are biased towards negative values ranging from -4% to 0%. The values of -4% obtained for XBTs manufactured on 1986 is agrees with the ‘cold’ XBT fall-rate bias identified and corrected after the study of H95. Note that the H95 correction was not applied to the XBT profiles used in this study. Most of the profiles show depth errors that are highly correlated with depth (Table 1, Column 6) suggesting a linear dependence with depth (Figure 3b, 2e, and 2h). This clear linear dependence indicates a bias in the processes represented by the  $A$  coefficient of the FRE, i.e. the balance of buoyancy and drag. Thus, the depth errors identified here are consistent with XBTs reaching an actual terminal velocity lower than  $A = 6.472 \text{ ms}^{-1}$ , i.e. a fall-rate bias. Note that the  $-Bt^2$  term in the FRE is much smaller than the  $At$  term because it is just a correction to account for the loss of mass and the increase in drag with depth. Last but not least, a clear year-dependence of this bias becomes evident when the depth error estimates from the different profiles are separated into the three groups of years (Figure 4a).

According to our analysis of the 52 co-located XBT/CTD pairs, the median depth bias has changed monotonically from  $(-3.77 \pm 0.57) \%$  to  $(-1.05 \pm 1.34) \%$  for XBTs manufactured in 1986 and 2008, respectively, with an intermediate value of  $(-2.72 \pm 0.50) \%$  for 1990-1995 (Table 1, Column 5). The  $1\sigma$  uncertainty intervals of these fall-rate bias estimates exhibit a slight overlap. However, the  $1\sigma$  bounds separate well below 500 m (Figure 4a), indicating that they represent robust changes in the fall-rate

characteristics of the XBT probes with 67% probability. The strong linear dependence of the depth errors confirms the hypothesis that these errors are related to variations in the fall-rate of the XBT probe, which indicates that the  $A$  coefficient in the FRE was inaccurate before 2008. The negative value of the bias estimates (Table 1, Column 5) indicates the percentage value by which the  $A$  coefficient of the FRE has to be increased in order to correct the XBT depths to agree with the CTD profiles.

#### *b) Temperature and start-up errors*

Unlike the depth errors, the temperature errors do not show statistically significant biases (Figure 4b), probably due to loss of thermistor accuracy. However the amplitude of the uncertainty envelopes, an estimate of the random errors in temperature, does not show a consistent evolution with time, i.e. the random errors of the XBTs manufactured in 2008 are larger than those manufactured during 1990-1995. Moreover, the median of the temperature errors does not exceed 0.03 °C, a much smaller value than the 0.1 °C accuracy of the thermistor. The depth distribution of the median-error shows a much larger and robust underestimation of the temperature in the seasonal thermocline, possibly related to the finite-time response of the XBT thermistor (Roemmich and Cornuelle 1987).

We also tested the possibility of surface offsets associated with start-up transients. These offsets can be estimated by computing the least-squares best-fit line of the depth errors, but allowing for a constant value at  $z = 0$ . The estimated median values of the implied surface errors are small, not significant, and with uncertainty within the 5 m specified by Sippican (Table 1, Column 7) indicating that there are no systematic biases

at the surface. During the PNE09 experiment the XBTs were carefully dropped from the depth specified by Sippican to minimize the effect of hydrodynamical transients not captured by the FRE, possibly explaining the absence of this type of errors, that could be more common in profiles collected from ships of opportunity.

### 3. Conclusions

Using a method that can estimate true XBT depths independent of temperature errors, we have found evidence of a ‘cold’ XBT fall-rate bias that has monotonically changed from  $(-3.77 \pm 0.57) \%$  to  $(-1.05 \pm 1.34) \%$  between 1986 and 2008. This work is the first study showing this year-dependence using a methodology that can unambiguously separate depth errors from ‘pure’ temperature errors. A rather large uncertainty is associated with these estimates due to the small number of profiles (between 12 and 21). However, the year-dependent variations in the fall-rate bias are statistically significant at the  $1\sigma$  confidence level below 500 m, where the effect of the fall-rate bias is larger. Our results for XBTs manufactured in 2008 also agree with results from experiments performed in 2007 (D. Snowden 2008, personal communication) showing that the original Sippican FRE coefficients may be more accurate than the H95 correction. Overall our results indicate that the changes in fall-rate characteristics of the XBT probe may be real with a 67% probability.

H95 analyzed XBT-CTD pairs collected in several experiments between 1985 and 1992. A total of 161 profiles obtained with T7 XBTs manufactured by Sippican were analyzed. Our estimates of a “cold” fall-rate bias of  $(-3.77 \pm 0.20) \%$  and of  $(-2.72 \pm 0.20) \%$  for XBTs manufactured in 1986 and in 1990-1995, respectively, bracket the -

3.52 % estimate obtained by H95 for the T7 model. H95 do not provided details on the manufacture dates of these XBTs, but if we assume that they were close to the date of the experiments, then our results are in agreement. The fall-rate bias found herein also shows a monotonic decrease with time, when the XBTs manufactured between 1990 and 1995 are separated into two groups of 9 XBTs for 1990-1991 and 12 for 1995. However, the change from  $(-2.72 \pm 0.50)$  % in 1990-1991 to  $(-2.49 \pm 0.55)$  % in 1995 is not statistically significant at the  $1\sigma$  confidence level.

No evidence of pure temperature biases were found, apart from a slight cold bias in the seasonal thermocline. However, since we used XBTs that exceeded the shelf life of the Thermistor, we cannot rule out the possibility that XBTs also suffer from temperature biases. A suggestion of a cold bias of about 0.1 °C in the seasonal thermocline in these profiles could have implications for studying trends in thermal stratification in response to global warming. Because XBTs dominate the earlier part of the climate record prior to 2000, and seem to measure a more diffuse seasonal thermocline, a spurious trend could be introduced when the XBT data are combined with data from more accurate Argo floats available since 2000.

Overall, our results indicate that the H95 correction was adequate for XBTs manufactured between 1986-1991, which is close to the 1985 to 1992 range of years covered by the experiments analyzed by H95. Moreover, our results also indicate that the H95 correction may have been no longer adequate as early as 1995, and is clearly inadequate for XBTs manufactured in 2008 when the original Sippican FRE gives smaller depth bias in agreement with previous studies (Wijffels et al. 2008; DiNezio and Goni 2010).



The results discussed herein have an immediate bearing on the discussion as to whether time-varying XBT biases are due to changes in the fall-rate bias or to are changes in a ‘pure’ temperature bias. Our results indicate that, at least for the 1986-2008 period, the hypothesis that the XBT errors are due to a time-varying fall-rate bias, as hypothesized by Wijfels et al. (2008), cannot be rejected. However, it is possible that XBT biases during the earlier part of the record, such as the large temperature biases during the late 1970s-early 1980s, are due to ‘pure’ temperature bias introduced by the strip-chart recorder as hypothesized by Gouretsky and Reseghetti (2010).

Once the fall-rate bias is corrected, the residual errors show no biases (Figure 4c). These residual errors estimate the random errors likely to result from the limitations of the FRE to capture the complex hydrodynamics of the descent of the probes. The  $1\sigma$  envelope of these errors has constant amplitude with depth of about 5 m, much smaller than the 2% specified by Sippican for depths below 250 m. This indicates that smaller uncertainty could be placed on XBT profiles if fall-rate biases are corrected. This could be achieved for future observations, for instance, if the XBTs had a pressure sensor activated at a given depth, ideally between 600 m and 700 m. Our analysis indicates that most of the XBT depth errors result from fall-rate variations, and thus are highly correlated with depth. Therefore, just one direct depth observation could be used to estimate the true fall-rate of each individual XBT probe and calibrate the FRE for each individual profile. XBTs were designed for naval applications that do not require the accuracy needed to detect global ocean warming. However, adding a single use pressure sensor would dramatically improve the accuracy of the XBT, rendering it more versatile for future climate applications.

372    **Acknowledgments**

373    We thank Rick Lumpkin for coordinating the co-located CTD and XBT casts during the  
374    2009 PIRATA Northeast extension cruise. This research was carried out in part under the  
375    auspices of the Cooperative Institute for Marine and Atmospheric Studies (CIMAS), a  
376    Joint Institute of the University of Miami and the National Oceanic and Atmospheric  
377    Administration (NOAA), Cooperative Agreement NA17RJ1226. P. N. DiNezio and G. J.  
378    Goni were supported by NOAA/AOML and the Ship of Opportunity Program (SOOP).  
379    The SOOP is funded by NOAA's Office of Climate Observations.

380

## References

- DiNezio, P. N. and G. J. Goni, 2010: Identifying and Estimating Biases Between XBT and Argo Observations Using Satellite Altimetry. *J. Atmos. Oceanic Technol.*, **27**, 226–240.
- Domingues, C. M., J. A. Church, N. J. White, P. J. Glecker, S. E. Wijffels, P. M. Barker, and J. R. Dunn, 2008: Improved estimates of upper-ocean warming and multi decadal sea-level rise. *Nature*, **453**, 1090–1093.
- Gouretski, V. and F. Reseghetti, 2010: On depth and temperature biases in bathythermograph data: Development of a new correction scheme based on analysis of a global ocean database. *Deep Sea Res. I*. doi:10.1016/j.dsr.2010.03.011
- Green, A. W., 1984: Bulk dynamics of the expendable bathythermograph (XBT). *Deep-Sea Res.*, **31**, 415–483.
- Hallock, Z. R. and W. J. Teague, 1992: The fall rate of the T-7 XBT. *J. Atmos. Oceanic Technol.*, **9**, 470–483.
- Hanawa, K. and H. Yoritaka, 1987: Detection of systematic errors in XBT data and their correction. *J. Oceanogr. Soc. Jpn.*, **32**, 68-76.
- Hanawa, K. and Y. Yoshikawa, 1991: Reexamination of depth error in XBT data. *J. Atmos. Oceanic Technol.*, **8**, 422-429.

399 Hanawa K. and T. Yasuda, 1992: New detection method for XBT depth error and  
 400 relationship between the depth error and coefficients in the depth-time equation,  
 401 *J. Oceanogr.*, **48**, 221-230.

402 Hanawa, K., P. Rual, R. Bailey, A. Sy, and M. Szabados, 1995: A new depth-time  
 403 equation for Sippican or TSK T-7, T-6 and T-4 expendable bathythermographs  
 404 (XBT). *Deep Sea Res. I*, **42**, 1423–1451.

405 Ishii, M. and M. Kimoto, 2009: Reevaluation of historical ocean heat content variations  
 406 with time-varying XBT and MBT depth bias corrections. *J. Oceanogr.*, **65**(3),  
 407 287-299.

408 Levitus, S., J. I. Antonov, T. P. Boyer, R. A. Locarnini, H. E. Garcia, and A. V.  
 409 Mishonov, 2009: Global ocean heat content 1955–2008 in light of recently  
 410 revealed instrumentation problems. *Geophys. Res. Lett.*, **36**, L07608.

411 Roemmich, D. and B. Cornuelle, 1987: Digitization and calibration of the expendable  
 412 bathythermograph. *Deep-Sea Res.*, **34**, 299–307.

413 Rual, P., 1991: XBT depth correction. Addendum to the Summary Report of the Ad Hoc  
 414 Meeting of the IGOSS Task Team on Quality Control for Automated Systems.  
 415 Marion, Massachusetts. U.S.A., June 1991, IOC/INF-888 Add., pp. 131-144.

416 Saunders, P. M., 1981: Practical conversion of pressure to depth. *J. Phys. Oceanogr.*,  
 417 **11**(4), 573–574.

418 Seaver, G. A. and S. Kuleshov, 1982: Experimental and analytical error of expendable  
 419 bathythermograph. *J. Phys. Oceanogr.*, **12**, 592–600.

420 Wijffels, S. E., J. Willis, C. M. Domingues, P. Barker, N. J. White, A. Gronell, K.  
421 Ridgway, and J. A. Church, 2008: Changing Expendable Bathythermograph Fall  
422 Rates and Their Impact on Estimates of Thermosteric Sea Level Rise. *J. Climate*,  
423 **21**, 5657–5672.

424 Willis, J. K., J. M. Lyman, G. C. Johnson, and J. Gilson, 2009: In Situ Data Biases and  
425 Recent Ocean Heat Content Variability. *J. Atmos. Oceanic Technol.*, **26**, 846–852.

426

## List of Figures

**Figure 1** – (top) Locations of co-located XBT/CTD casts in the northeastern tropical Atlantic.....25

**Figure 2** – (a) Temperature profiles and (b) their vertical gradients obtained from a CTD cast (blue) and an XBT cast (red) on the equator at 23°W. The green lines in (a) and (b) are the adjusted temperature profile and its vertical gradient, resulting from adjustment of the vertical gradient of the XBT profile (red) in order to maximize local correlation with the vertical gradient of the CTD profile. The overall correlation between the vertical gradients of the XBT and CTD profiles goes from 0.72 to 0.97 once the XBT profile is locally adjusted. (c) Maximum correlation coefficient between the XBT and CTD gradient within a 50 m depth window centered at each depth. (d) Vertical shift of the vertical gradient of the XBT profile that maximizes the local correlation between the CTD and XBT gradients. Positive values indicate an upward shift. ....26

**Figure 3** – (left) Temperature profiles obtained from CTDs (blue) and XBTs (red) manufactured in (a) 1986, (d) 1990-1995, and (g) 2008. (center) Differences between the depth estimated by the XBT fall-rate equation (FRE) with the original Sippican coefficients minus the true XBT depth estimated using the methodology described in the text (gray dots). The profiles are separated according to the manufacture date of the XBTs: (b) 1986, (e) 1990-1995, and (h) 2008. The median value of the depth differences is shown in red. Depth differences are in m. The dotted lines determine the XBT depth error specified by Sippican: 2% of depth or 5

m, whichever is larger. (right) XBT minus CTD temperature as function of depth after the depth of the XBT profile is adjusted using the methodology described in the text (gray dots). The profiles are separated according to the manufacture date of the XBTs: (c) 1986, (f) 1990-1995, and (i) 2008. The median value of the temperature differences is shown in red. Temperature differences are in °C.....27

**Figure 4** – Vertical profiles of (a) depth errors, (b) temperature errors, and (c) depth errors after fall-rate corrections (solid line) and uncertainty interval (thin lines) of temperature profiles obtained with XBTs manufactured in 1986 (black), 1990-1995 (red), and 2008 (blue). In all panels the depth-dependent error is the median difference among all profiles with a given manufacture date, and the uncertainty interval is their standard deviation. The depth differences are the depth estimated by the XBT fall-rate equation (FRE) using the original Sippican coefficients minus the true depth estimated using the methodology described in the text. Depth differences are in m. Temperature differences are in °C. The dotted lines in (c) determine the XBT depth error specified by Sippican: 2% of the depth or 5 m, whichever is larger. ....29

465    **List of Tables**

466    **Table 1** – Depth and temperature biases for XBTs manufactured on different years  
467        during the 1980s, 1990s, and 2000s .....30

468

469



Figures

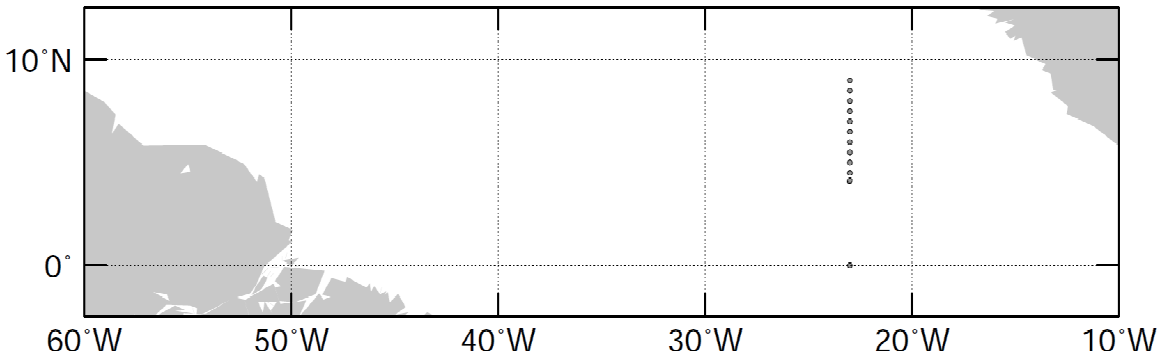
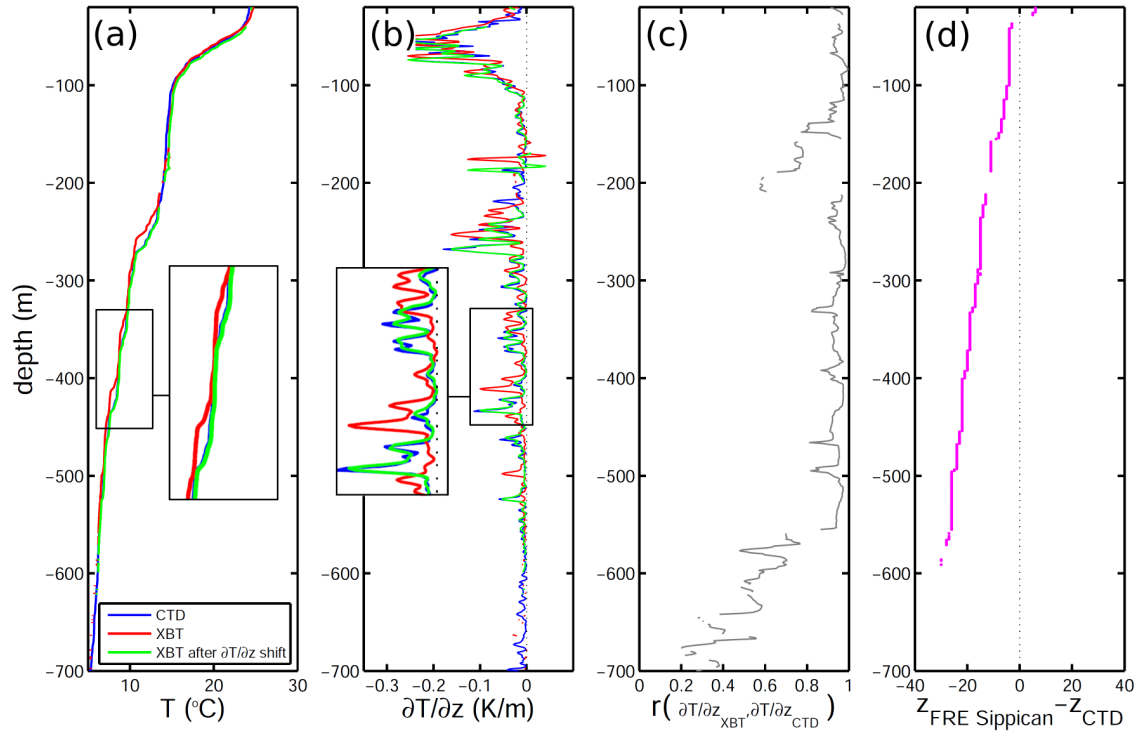


**Figure 1 – (top)** Locations of co-located XBT/CTD casts in the northeastern tropical Atlantic



473

474 **Figure 2** – (a) Temperature profiles and (b) their vertical gradients obtained from a CTD cast  
 475 (blue) and an XBT cast (red) on the equator at 23°W. The green lines in (a) and (b) are the  
 476 adjusted temperature profile and its vertical gradient, resulting from adjustment of the vertical  
 477 gradient of the XBT profile (red) in order to maximize local correlation with the vertical gradient of  
 478 the CTD profile. The overall correlation between the vertical gradients of the XBT and CTD  
 479 profiles goes from 0.72 to 0.97 once the XBT profile is locally adjusted. (c) Maximum correlation  
 480 coefficient between the XBT and CTD gradient within a 50 m depth window centered at each  
 481 depth. (d) Vertical shift of the vertical gradient of the XBT profile that maximizes the local  
 482 correlation between the CTD and XBT gradients. Positive values indicate an upward shift.

483

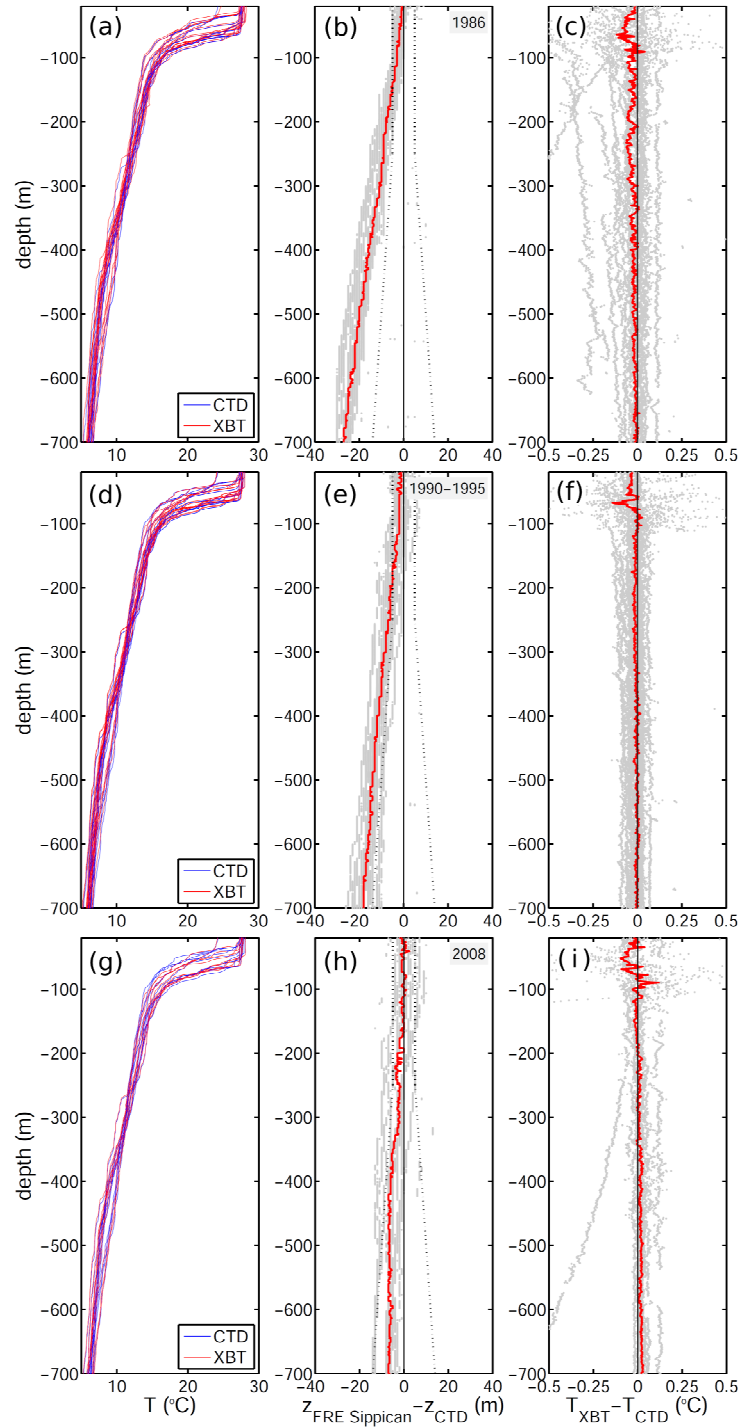
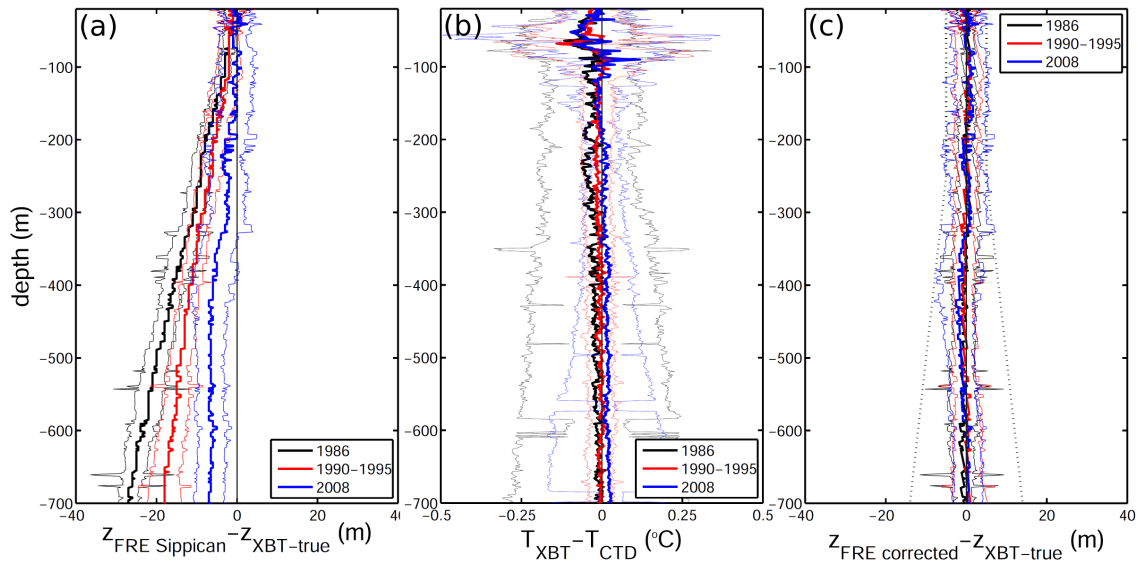


**Figure 3** – (left) Temperature profiles obtained from CTDs (blue) and XBTs (red) manufactured in (a) 1986, (d) 1990-1995, and (g) 2008. (center) Differences between the depth estimated by the XBT fall-rate equation (FRE) with the original Sippican coefficients minus the true XBT depth

487 estimated using the methodology described in the text (gray dots). The profiles are separated  
488 according to the manufacture date of the XBTs: (b) 1986, (e) 1990-1995, and (h) 2008. The  
489 median value of the depth differences is shown in red. Depth differences are in m. The dotted  
490 lines determine the XBT depth error specified by Sippican: 2% of depth or 5 m, whichever is  
491 larger. (right) XBT minus CTD temperature as function of depth after the depth of the XBT profile  
492 is adjusted using the methodology described in the text (gray dots). The profiles are separated  
493 according to the manufacture date of the XBTs: (c) 1986, (f) 1990-1995, and (i) 2008. The median  
494 value of the temperature differences is shown in red. Temperature differences are in °C.

495

495



496

497 **Figure 4** – Vertical profiles of (a) depth errors, (b) temperature errors, and (c) depth errors after  
 498 fall-rate corrections (solid line) and uncertainty interval (thin lines) of temperature profiles  
 499 obtained with XBTs manufactured in 1986 (black), 1990-1995 (red), and 2008 (blue). In all panels  
 500 the depth-dependent error is the median difference among all profiles with a given manufacture  
 501 date, and the uncertainty interval is their standard deviation. The depth differences are the depth  
 502 estimated by the XBT fall-rate equation (FRE) using the original Sippican coefficients minus the  
 503 true depth estimated using the methodology described in the text. Depth differences are in m.  
 504 Temperature differences are in °C. The dotted lines in (c) determine the XBT depth error  
 505 specified by Sippican: 2% of the depth or 5 m, whichever is larger.

506

506 **Tables**

XBT manufa cture date	Number of profiles	Correlation coefficient between $\partial T/\partial z_{CTD}(z)$ and $\partial T/\partial z_{XBT}(z)$		Depth bias		Surface offset (m)	Temperatur e bias (°C)
		After depth adjustment	Before depth adjustment	Magnitude (%)	Correlation of depth dependence		
1986	19	$0.79 \pm 0.12$	$0.97 \pm 0.01$	$-3.77 \pm 0.57$	$-0.98 \pm 0.07$	$0.20 \pm 1.54$	$-0.03 \pm 0.17$
1990- 1995	21	$0.77 \pm 0.15$	$0.97 \pm 0.01$	$-2.72 \pm 0.50$	$-0.96 \pm 0.08$	$-0.56 \pm 3.03$	$-0.01 \pm 0.04$
2008	12	$0.74 \pm 0.15$	$0.97 \pm 0.02$	$-1.05 \pm 1.34$	$-0.61 \pm 0.46$	$0.58 \pm 4.25$	$0.01 \pm 0.08$

507 **Table 1** – Depth and temperature biases for XBTs manufactured on different years during the  
508 1980s, 1990s, and 2000s

509